



Fabrication and structural properties of flower-like TiO₂ nanorod array films grown on glass substrate without FTO layer

M.Z. Musa^{a,f}, M.H. Mamat^{a,b,*}, N. Vasimalai^c, I.B. Shameem Banu^c, M.F. Malek^b, M.K. Ahmad^d, A.B. Suriani^e, A. Mohamed^e, M. Rusop^{a,b}

^a NANO-ElecTronic Centre (NET), Faculty of Electrical Engineering, Universiti Teknologi MARA (UiTM), 40450 Shah Alam, Selangor, Malaysia

^b NANO-SciTech Centre (NST), Institute of Science (IOS), Universiti Teknologi MARA (UiTM), 40450 Shah Alam, Selangor, Malaysia

^c School of Physical and Chemical Sciences, B.S. Abdur Rahman Crescent Institute of Science & Technology, Vandalur, Chennai 600 048, India

^d Microelectronic and Nanotechnology-Shamsuddin Research Centre, Faculty of Electrical and Electronic Engineering, Universiti Tun Hussein Onn Malaysia, 86400 Batu Pahat, Johor, Malaysia

^e Nanotechnology Research Centre, Faculty of Science and Mathematics, Universiti Pendidikan Sultan Idris (UPSI), 35900 Tanjung Malim, Perak, Malaysia

^f Faculty of Electrical Engineering, Universiti Teknologi MARA Cawangan Pulau Pinang, 13500 Permatang Pauh, Pulau Pinang, Malaysia

ARTICLE INFO

Article history:

Received 26 March 2020

Received in revised form 28 April 2020

Accepted 29 April 2020

Available online 30 April 2020

Keywords:

Semiconductors

TiO₂ flower-like nanorod array

Sol-gel preparation

Structural properties

Humidity sensor

ABSTRACT

For the first time, flower-like titanium dioxide (TiO₂) nanorod array (TFNA) films were grown on sputtered TiO₂ seed layer-coated glass substrate without fluorine-doped tin oxide (FTO) layer during 1–5 h immersions. The optimum immersion time was 4 h, which produced a dense TFNA structure with thickness of 19 μm. X-ray diffraction results revealed that the TFNA were of a tetragonal rutile phase. A humidity sensor, fabricated using the prepared sample, showed excellent humidity sensor performance, with sensitivity reaching up to 196. The results indicate that the prepared TFNA films are promising material for humidity sensing applications.

© 2020 Elsevier B.V. All rights reserved.

1. Introduction

Titanium dioxide (TiO₂) nanostructures are actively being explored for various applications, such as solar cells, photoanodes, photocatalysts and sensors. The nanostructures help to improve the performance of the devices through increased surface area and efficient carrier transfer. Various methods have been employed to prepare TiO₂ nanostructures, including electrochemical anodisation, electrospinning and hydrothermal methods. To grow TiO₂ nanostructures, either fluorine-doped tin oxide (FTO) or indium-doped tin oxide (ITO) glasses are usually required. Yusoff et al. [1] have demonstrated the preparation of TiO₂ nanorods on FTO-coated substrates using an immersion method, while Qi et al. [2] have produced TiO₂ nanorods on ITO-coated substrates using hydrothermal methods. Sawant et al. [3] and Shalini et al. [4] also used FTO glass to grow TiO₂ nanostructures. However, the use of FTO and ITO substrates could limit the application of TiO₂, which occasionally requires a pristine TiO₂ structure without the conductive layer. Furthermore, FTO- and ITO-coated substrates are rela-

tively expensive. Therefore, it is important to grow TiO₂ nanostructures on substrates with FTO or ITO independency.

Herein, we explore the possibility of producing TiO₂ flower-like nanorod array (TFNA) structures using a one-step aqueous chemical immersion method with a sputtered TiO₂ layer as a seed layer. To the best of our knowledge, there have been few reports on the synthesis of TFNA without using FTO or ITO substrates. This TFNA film enables the fabrication of a metal-semiconductor-metal (MSM)-type humidity sensor with high sensitivity.

2. Experimental

A TiO₂ seed layer was prepared on a glass substrate by RF sputtering (SNTEK) using TiO₂ target (99.99% purity) at a power of 200 W under 20sccm argon and 5sccm oxygen gas flow. The chamber pressure was maintained at 5mTorr during deposition using an automated adjustable throttle valve. The deposition time was fixed at 6 h to achieve an average thickness of 370 nm. A solution for the immersion method was prepared by mixing deionised (DI) water and hydrochloric acid (HCl) in a Schott bottle at 1:1 ratio for 10 min before adding 0.07 M of tetrabutyl titanate (97%, Sigma-Aldrich). The solution was then stirred for another 50 min. Glass

* Corresponding author.

E-mail address: mhmamat@uitm.edu.my (M.H. Mamat).

substrate with TiO_2 seed layer was inserted into the solution with the seed layer facing upward. Next, the Schott bottle was put inside an oven at 150°C for immersion time from 1 to 5 h. After the immersion process, the samples were rinsed with DI water and annealed at 450°C for 1 h. For the measurement of humidity sensor properties, silver (Ag) metal contact was deposited on top of

the samples using thermal evaporator (ULVAC). The final structure of the samples is illustrated in Fig. 1(a). The structural characterisation was carried out using field-emission scanning electron microscopy (FESEM, JEOL JSM-7600F), X-ray diffraction (XRD, PANalytical X'pert PRO) and micro-Raman spectroscopy (Horiba Jobin Yvon-79 DU420A-OE-325, 514 nm Ar laser). The humidity

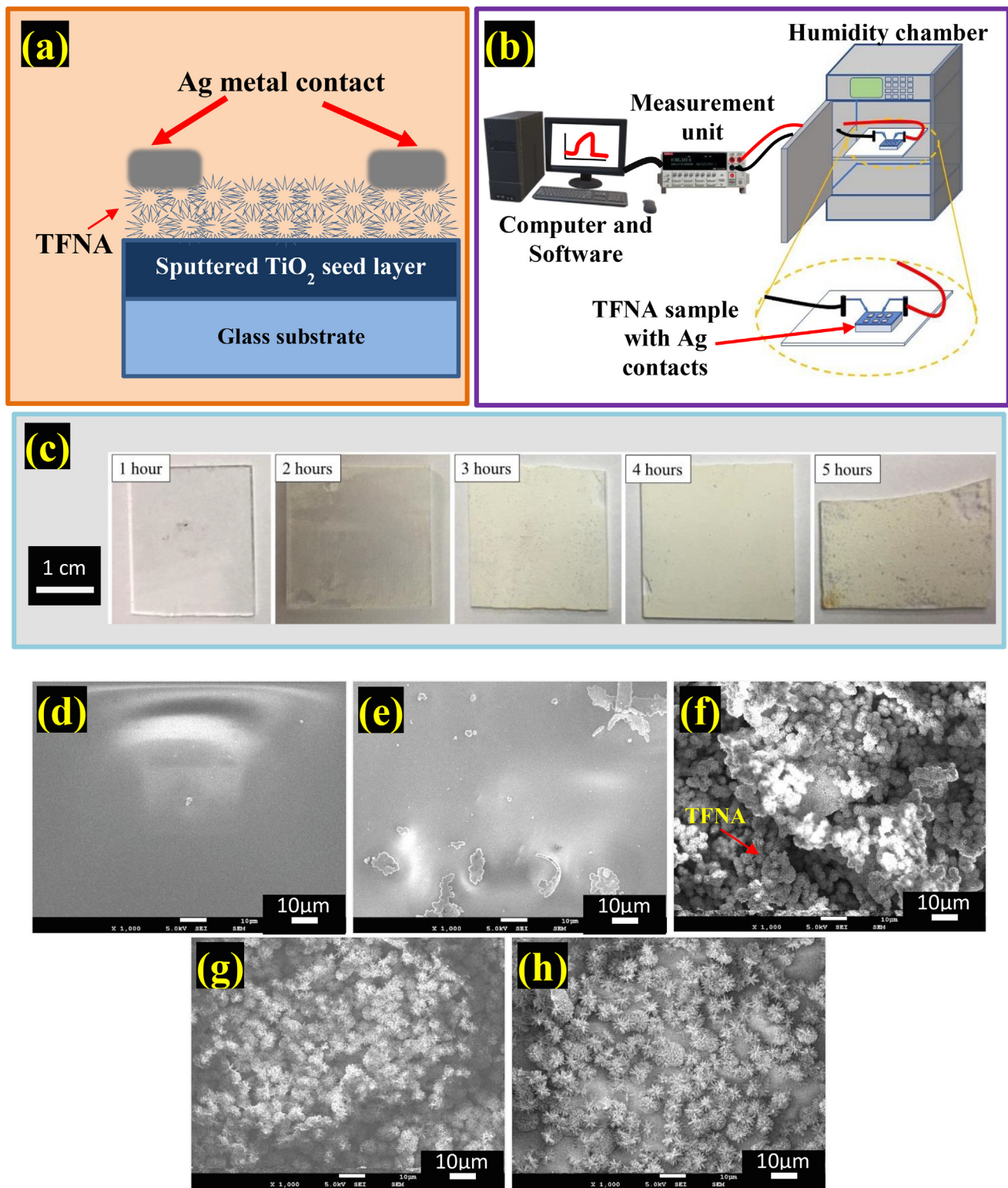


Fig. 1. (a) Configuration of a TFNA film-based humidity sensor.(b) Schematic of the humidity sensing measurement setup. (c) Photo images of TFNA at various times. (d-h) FESEM images of TFNA at different immersion times of (d)1h, (e) 2h, (f) 3h, (g) 4h and (h) 5h.

sensor performance was measured inside a humidity chamber (ESPEC-SH261) using the sensor measurement system (Keithley 2400). The humidity sensing measurement setup is depicted in Fig. 1(b).

3. Results and discussion

3.1. Structural properties

The photo images of the prepared samples are depicted in Fig. 1(c). At the immersion time of 1 h, the glass substrate remained

completely transparent, while small patches of white colored layer were visible at the growth time of 2 h. Further increase in the immersion time to 3–5 h produced uniform white layers with different densities. The FESEM images of the prepared samples are shown in Fig. 1(d–h). No formation of TiO_2 nanostructures was observed at the initial immersion time of 1 h (Fig. 1[d]). At 2 h, as depicted in Fig. 1(e), only small patches of TiO_2 nanostructures were observed on the substrate, indicating that the formation of TFNA had just started. Increasing the deposition time to 3 h, the formation of TFNA was uniform across the substrate surface, as shown in Fig. 1(f). Increasing the deposition time further to 4 h

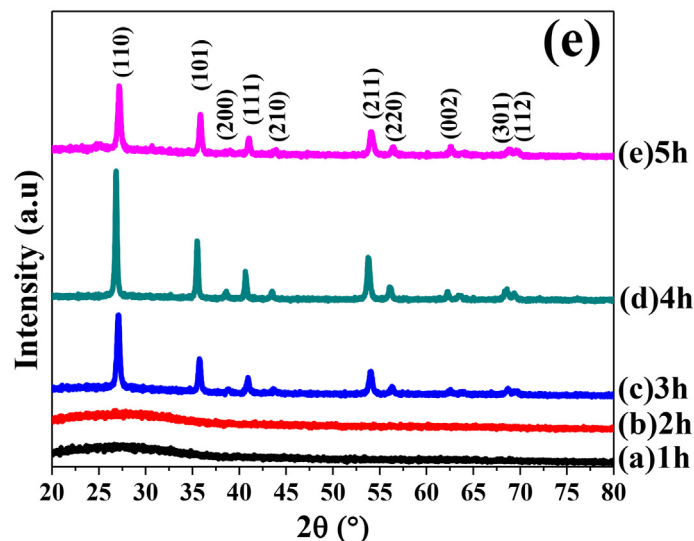
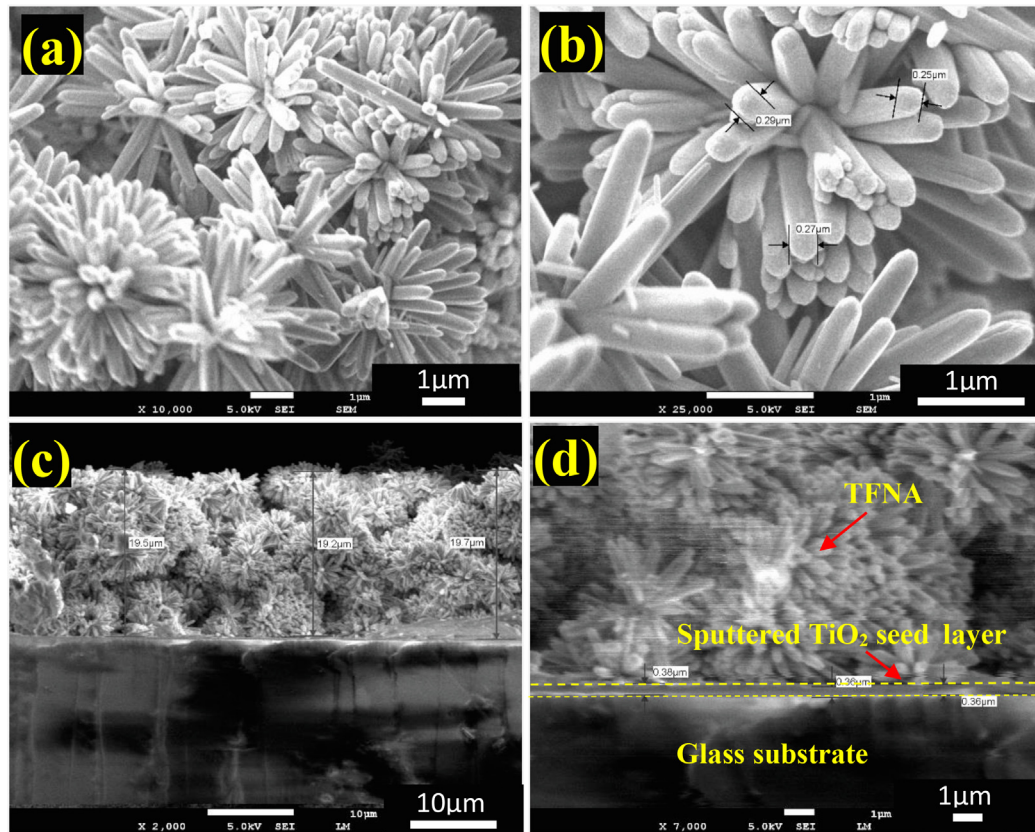
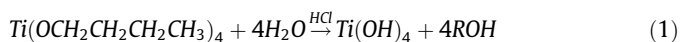


Fig. 2. (a–b) Magnified images of TFNA(4 h) at a magnification of (a) 10,000 × and (b) 25,000 ×. (c–d) Cross-section of TFNA(4 h) at a magnification of (c) 2,000 × and (d) 7,000 ×. (e) XRD patterns of TFNA at different immersion times.

increased the denseness of the structure, as shown in Fig. 1(g). However, as the immersion time reached 5 h, the denseness of the TFNA seemed to decrease in Fig. 1(h), which was possibly due to dissolution process of the nanostructures in the acidic medium.

Further investigation was conducted for the TFNA at 4 h. Increased magnification images revealed dense TFNA that resembled a dandelion-like structure, as shown in Fig. 2(a-b). Each of the TFNA structures consisted of nanorods with an average diameter of 0.27 μm . Cross-sectional FESEM views were also taken and are shown in Fig. 2(c-d). The images show that the average thickness of the seed layer was 0.37 μm , while the TFNA structure had a thickness of 19 μm .

The growth mechanism of TFNA could be explained by the following chemical reactions:



Initially, a hydrolysis reaction eliminated four carbon atoms from a titanium precursor, forming titanium hydroxyl. This was followed by a condensation reaction, which produced TiO_2 and water. The presence of HCl was crucial to stabilise the reactions and prevent the formation of large aggregates [1]. The basic building block of TiO_2 based compounds was the TiO_6 octahedra. In the titanium precursor, tetrabutyl titanate and highly electronegative OR^- ligands shared the titanium's four valence electrons, which were located at the equatorial hybrid orbitals. The remaining two axial orbitals were left vacant. With the addition of water, a hydrolysis reaction occurred and the OR^- ligands were replaced by highly nucleophilic OH^- (hydroxo) groups originated from the dissociation of H_2O . Meanwhile, the OR^- ligand underwent protonation to produce ROH (alcohol). Vacant axial orbitals would then

receive an electron pair from the water molecules, forming a neutral hydroxo-aquo $[\text{Ti}(\text{OH})_4(\text{OH}_2)_2]^0$ complex. These neutral complexes tend to aggregate to form amorphous TiO_2 due to van der Waals attraction forces. However, this could be avoided with the addition of HCl. The acid reduced the initial concentration of dissociated hydroxy groups $\text{c}[\text{OH}^-]$ in the solution and protonated OH^- ligands in Ti-hydroxo complex, which increased electrostatic repulsion between the complexes and prevented their immediate condensation [5]. The TFNA, which comprised of interconnected three-dimensional TiO_2 architectures, could be produced in highly acidic medium of HCl under supersaturation conditions. The growth mechanism is further discussed in [supplementary material](#).

XRD patterns of the samples are shown in Fig. 2(e). The samples at 1 h and 2 h showed no observable peak. This was likely due to the amorphous phase of the seed layer and the absence of TFNA in both samples, as observed in the FESEM images. Multiple peaks were detected for samples immersed at 3–5 h, pointing to a tetragonal rutile TiO_2 structure (JCPDS No.01–072–1148). The rutile phase of the sample was further confirmed by Raman analysis, presented in [supplementary material](#). The TFNA at 4 h showed the strongest XRD peaks, indicating that high crystallinity was achieved for this sample. The crystallite size, lattice parameters, microstrain and dislocation density were estimated based on the XRD pattern and are presented in the [supplementary material](#). Furthermore, the TFNA at 4 h showed the lowest microstrain and dislocation density values.

3.2. Humidity sensor performance

The humidity sensing response of the prepared samples at 5 V-bias are shown in Fig. 3(a). It was observed that, in all samples, the current value increased steadily as the humidity level was increased from 40 to 90%RH and then decreased swiftly when the humidity was reduced from 90 to 40%RH. The sensitivity value of the humidity sensor was defined using the following equation:

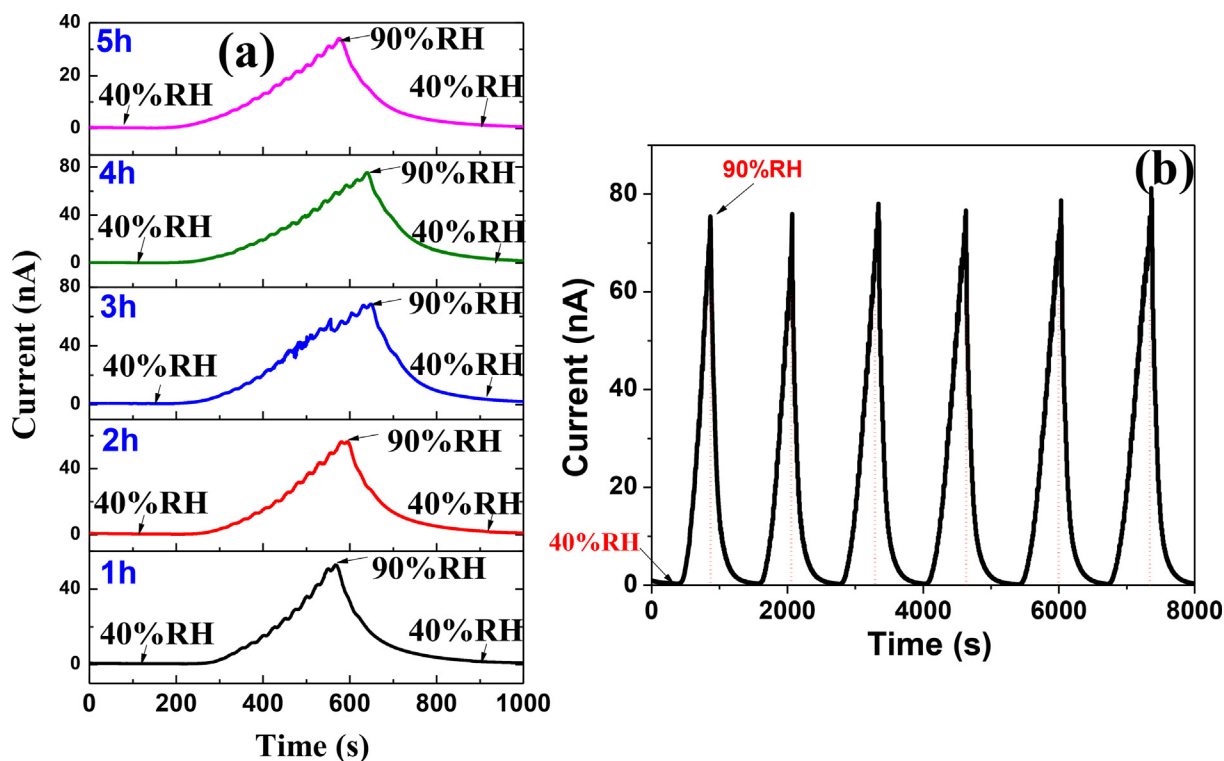


Fig. 3. (a) Humidity sensing response of TFNA at different immersion times.(b) Reliability test of humidity sensing for TFNA(4 h).

$$S = \frac{R_{40}}{R_{90}} \quad (4)$$

where R_{40} is the stabilised resistance at 40%RH and R_{90} is the resistance at 90%RH. The calculated sensitivity values for TFNA at 1, 2, 3, 4 and 5 h were 137, 144, 178, 196 and 89, respectively. The sensitivity value slowly increased with the increase in immersion time, reaching the highest sensitivity value at 196 for the sample immersed for 4 h, before decreasing significantly afterwards. This result could be explained by referring to the humidity sensing mechanism and the thin film's structural properties. The humidity sensing mechanism is discussed in the [supplementary material](#). Since the sample immersed for 4 h had the highest TFNA denseness among the samples, it was conceivable that its surface could absorb more water molecules, making it more sensitive compared to the other samples. In addition, the TFNA at 4 h showed the lowest microstrain and dislocation density values, which contributed to the improved humidity sensing performance. A six-cycle reliability test was conducted for the TFNA at 4 h and the result is shown in [Fig. 3\(b\)](#). The device performed reasonably well, with a consistent current value in all cycles. No significant drop in the current value was observed in any of the cycles.

4. Conclusion

A novel method of preparing a TFNA on glass substrate has been realised by utilising sputtered TiO_2 as the seed layer. TFNA was observed after 3 h of immersion time, having a rutile phase. The fabricated humidity sensor based on TFNA exhibited excellent humidity sensing capability, with the sample immersed for 4 h achieving a sensitivity value of 196 and showing stable current values in the reliability test. In conclusion, the fabricated TFNA is a promising material for humidity sensing.

Declaration of Competing Interest

The authors declare that they have no known competing financial interests or personal relationships that could have appeared to influence the work reported in this paper.

Acknowledgments

The authors would like to acknowledge Ministry of Higher Education Malaysia under FRGS research grant (FRGS/1/2018/TK04/UiTM/02/23) and Indian Government (ASEAN-India Research&Training Fellowship [RTF/2019/000103]). The authors also acknowledge the contribution of Faculty of Electrical Engineering and Institute of Research Management and Innovation (IRMI), UiTM.

Appendix A. Supplementary data

Supplementary data to this article can be found online at <https://doi.org/10.1016/j.matlet.2020.127902>.

References

- [1] M.M. Yusoff, M.H. Mamat, M.F. Malek, A.B. Suriani, A. Mohamed, M.K. Ahmad, et al., Growth of titanium dioxide nanorod arrays through the aqueous chemical route under a novel and facile low-cost method, *Mater. Lett.* 164 (2016) 294–298.
- [2] W. Qi, J. Du, Y. Peng, W. Wu, Z. Zhang, X. Li, et al., Hydrothermal synthesis of TiO_2 nanorods arrays on ITO, *Mater. Chem. Phys.* 207 (2018) 435–441.
- [3] J.P. Sawant, R.B. Kale, Surfactant mediated TiO_2 photoanodes and $\text{Cu}_2\text{ZnSnS}_4$ counter electrodes for high efficient dye sensitized solar cells, *Mater. Lett.* 265 (2020) 127407.
- [4] S. Shalini, R. Balasundaraprabhu, T. Satish Kumar, N. Muthukumarasamy, S. Prasanna, K. Sivakumaran, et al., Enhanced performance of sodium doped TiO_2 nanorods based dye sensitized solar cells sensitized with extract from petals of *Hibiscus sabdariffa* (Roselle), *Mater. Lett.* 221 (2018) 192–195.
- [5] V. Jordan, U. Javornik, J. Plavec, A. Podgornik, A. Rečnik, Self-assembly of multilevel branched rutile-type TiO_2 structures via oriented lateral and twin attachment, *Sci. Rep.* 6 (2016) 24216.